ARTHRITIS & RHEUMATOLOGY
Vol. 67, No. 8, August 2015, pp 2061–2070
DOI 10.1002/art.39158

Shared Epitope–Antagonistic Ligands

A New Therapeutic Strategy in Mice With Erosive Arthritis

Song Ling,[1] Ying Liu,[1] Jiaqi Fu,[1] Alessandro Colletta,[1] Chaim Gilon,[2] and Joseph Holoshitz[1]

Objective. **The mechanisms underlying bone damage in rheumatoid arthritis (RA) are incompletely understood. We recently identified the shared epitope (SE), an HLA–DRB1–coded 5–amino acid sequence motif carried by the majority of RA patients as a signal transduction ligand that interacts with cell surface calreticulin and accelerates osteoclast (OC)–mediated bone damage in collagen-induced arthritis (CIA). Given the role of the SE/calreticulin pathway in arthritis-associated bone damage, we sought to determine the therapeutic targetability of calreticulin.**

Methods. **A library of backbone-cyclized peptidomimetic compounds, all carrying an identical core DKCLA sequence, was synthesized. The ability of these compounds to inhibit SE-activated signaling and OC differentiation was tested in vitro. The effect on disease severity and OC-mediated bone damage was studied by weekly intraperitoneal administration of the compounds to DBA/1 mice with CIA.**

Results. **Two members of the peptidomimetics library were found to have SE-antagonistic effects and antiosteoclast differentiation effects at picomolar concentrations in vitro. The lead mimetic compound, designated HS(4-4)c Trp, potently ameliorated arthritis and bone damage in vivo when administered in picogram doses to mice with CIA. Another mimetic analog, designated HS(3-4)c Trp, was found to lack activity, both in vitro and in vivo. The differential activity of the 2 analogs depended on minor differences in their respective ring sizes and correlated with distinctive geometry when computationally docked to the SE binding site on calreticulin.**

Conclusion. **These findings identify calreticulin as a novel therapeutic target in erosive arthritis and provide sound rationale and early structure/activity relationships for future drug design.**

Despite the advent of biologic agents, preventing bone damage in rheumatoid arthritis (RA) remains a challenging endeavor. Due to insufficient understanding of the mechanisms that trigger RA onset and determine disease severity, most current and emerging drugs are targeted at generic "downstream" immune pathways or inflammatory cytokines. As a result, drug failure and/or side effects are all too common.

The etiology and pathogenesis of RA are incompletely understood. However, it has long been observed that the majority of RA patients carry HLA–DRB1 alleles that code a 5–amino acid sequence motif called the "shared epitope" (SE) in region 70–74 of the DRβ chain (1). The SE not only confers a higher risk of RA, but it also increases the likelihood of developing more severe disease. SE-coding HLA–DRB1 alleles are associated with earlier disease onset and accelerated bone damage (2–5). Furthermore, there is evidence of a gene-dose effect, where the extent of bone destruction in RA correlates positively with the number of SE-coding HLA–DRB1 alleles (3–5).

The contents of this article are solely the responsibility of the authors and do not necessarily represent the official views of the National Institutes of Health.

Supported by the NIH (National Institute of General Medical Sciences grant 5R01-GM-088560, National Center for Research Resources grant UL 1-RR-024986, and National Institute of Arthritis and Musculoskeletal and Skin Diseases grants 5R01-AR-059085, 3R01-AR-059085-03S1, and T32-AR-07080).

[1]Song Ling, PhD, Ying Liu, MD, Jiaqi Fu, PhD, Alessandro Colletta, BS, Joseph Holoshitz, MD: University of Michigan School of Medicine, Ann Arbor; [2]Chaim Gilon, PhD: The Hebrew University of Jerusalem, Jerusalem, Israel.

Drs. Ling and Liu contributed equally to this work.

Drs. Ling, Gilon, and Holoshitz are named inventors on US patents for technologies related to rheumatoid arthritis, for which they receive no licensing fees. The patents are owned by the University of Michigan and The Hebrew University of Jerusalem.

Address correspondence to Joseph Holoshitz, MD, Division of Rheumatology, University of Michigan, 5520D MSRB1, 1150 West Medical Center Drive, Ann Arbor, MI 48109-5680. E-mail: jholo@umich.edu.

Submitted for publication September 17, 2014; accepted in revised form April 9, 2015.

The underlying mechanisms by which the SE affects susceptibility to, or the severity of, RA are unknown. We have recently identified the SE as a signal transduction ligand that binds to a well-defined site on cell surface calreticulin (6) in a strictly allele-specific manner and activates nitric oxide–mediated signaling (7–11), with resultant enhanced osteoclast (OC) differentiation and activation both in vitro and in vivo (12,13).

OC-mediated bone damage is a common and unfortunate outcome in RA (14,15). In addition to juxtaarticular bone erosion, RA patients also experience periarticular and systemic osteoporosis (16). The common mechanism underlying these pathologic changes of bone is believed to involve dysregulation of the balance between bone formation and resorption due to excessive cellular activity of OCs (17) as a result of intricate cross-talk with other cells in the synovium that produce RANKL (18–20).

In previous studies, we demonstrated that the SE ligand has a dual enhancing effect on OC differentiation and activation in vitro: an indirect effect through polarization toward RANKL-expressing Th17 cells and a direct differentiation effect on OC precursors. When administered in vivo to mice with collagen-induced arthritis (CIA), the SE ligand was shown to increase joint swelling, abundance of active OCs in synovial tissue, and erosive bone damage (12,13).

Given the emerging evidence that the SE acts as a signal transduction ligand that directly contributes to bone damage in arthritis, we explored ways to specifically inhibit this pathway. Here we describe a peptidomimetic SE-antagonistic ligand (SEAL) with highly potent antiosteoclastogenic and antiarthritic effects. These findings suggest that targeting the SE-activated pathway might be a useful therapeutic strategy.

MATERIALS AND METHODS

Reagents, peptidomimetics, cells, and mice. Ficoll-Paque, 4,5-diaminofluorescein diacetate (DAF-2-DA), macrophage colony-stimulating factor (M-CSF), RANKL, chicken type II collagen, and Freund's complete adjuvant (CFA) were purchased from sources described previously (13). All other commercial reagents were purchased from Sigma. Linear 5-mer peptides DKCLA, QKCLA, and DERAA, as well as 15-mer peptides 65–79*0401 (KDLLEQKRAAVDTYC) and 65–79*0404 (KDLLEQRRAAVDTYC), were synthesized and purified (>90%) as described elsewhere (9,10). The urea backbone cyclic peptidomimetics, designated generically as HS(m-n)c Trp, were synthesized according to a previously described procedure (21,22) using various alloc-protected glycine building units, where m represents the number of methylene groups in the *N*-alkyl chain on the glycine building unit at position 2, and n represents the number of methylene groups in the *N*-alkyl chain on the glycine building unit at position 6. A tryptophan residue at position 1 was used for tracing and quantification.

The isolation of human peripheral blood mononuclear cells (PBMCs) and mouse primary bone marrow cells (BMCs) and the culture of M1 fibroblasts have previously been described (13).

DBA/1 mice (6–10 weeks old) were purchased from The Jackson Laboratory. Mice were maintained and housed at the Unit for Laboratory Animal Medicine facility at the University of Michigan. All experiments were performed in accordance with protocols approved by the University Committee on Use and Care of Animals.

Surface plasmon resonance (SPR) analysis. A Biacore 2000 biosensor system was used to assay the interaction between soluble ligands and recombinant mouse calreticulin (6,11). SPR assay is based on a biosensor chip with a Dextran-coated gold surface that is coated with a covalently immobilized protein. Binding interactions between an injected ligand (the "analyte") and the immobilized protein result in SPR signals that are directly proportional to the amount and molecular mass of the ligand. Results are read in real time as resonance units (RU).

Before use, biosensor chips CM5 (Biacore) were preconditioned in water at 100 μl/minute by applying 2 consecutive 20-μl pulses of 50 m*M* NaOH, followed by 10 m*M* HCl, and finally 0.1% sodium dodecyl sulfate. The CM5 surface was activated by a 7-minute injection of 200 m*M* 1-ethyl-3-(3-dimethylaminopropyl) carbodiimide hydrochloride in 50 m*M* *N*-hydroxysuccinimide. Purified calreticulin was immobilized by standard primary amine coupling at 25°C in HBS-EP buffer (10 m*M* HEPES, pH 7.4, 150 m*M* NaCl, 1 m*M* EDTA, and 0.005% surfactant P20), at a flow rate of 10 μl/minute. The protein was injected manually at a concentration of 100 μg/ml until approaching 5,500 RU. The remaining activated groups were blocked by ethanolamine (1*M*).

Binding assays were performed at 25°C in a binding buffer (10 m*M* HEPES, pH 7.4, 50 m*M* KCl, 0.5 m*M* $CaCl_2$, 100 μ*M* $ZnCl_2$, and 0.005% surfactant P20) at a flow rate of 10 μl/minute. Ligands were applied to the analyte at various concentrations. The RU signal intensity at a given molar concentration is proportional to the molecular mass of the analyte. Accordingly, when a competitive small ligand is mixed with a larger ligand, a drop in the signal relative to the RU produced by the latter ligand alone is observed. This characteristic was used in our study to determine the competitive inhibition of the binding of the 15-mer peptides 65–79*0401 (MW 1,751 daltons) or 15-mer peptide 65–79*0404 (MW 1,751 daltons) to calreticulin by the 5-mer linear peptide DKCLA (MW 590 daltons) or the cyclic DKCLA (cDKCLA) mimetic (MW 902 daltons). All SPR data were calculated using the BIAevaluation version 3.0.1 program (Biacore).

In vitro assays. Nitric oxide signal transduction assays were performed using the nitric oxide probe DAF-2-DA. The fluorescence level was recorded every 5 minutes over a period of 500 minutes using a Fusion αHT system (PerkinElmer Life Sciences) at an excitation wavelength of 488 nm and emission wavelength of 515 nm. In vitro assays for OC differentiation were performed using primary mouse BMCs isolated from femurs and tibias or using human PBMCs isolated from healthy blood donors. Mouse BMCs were cultured in 48-well plates (2×10^5/well) α-minimum in essential medium supplemented with 10% fetal bovine serum, 100 units/ml of penicillin,

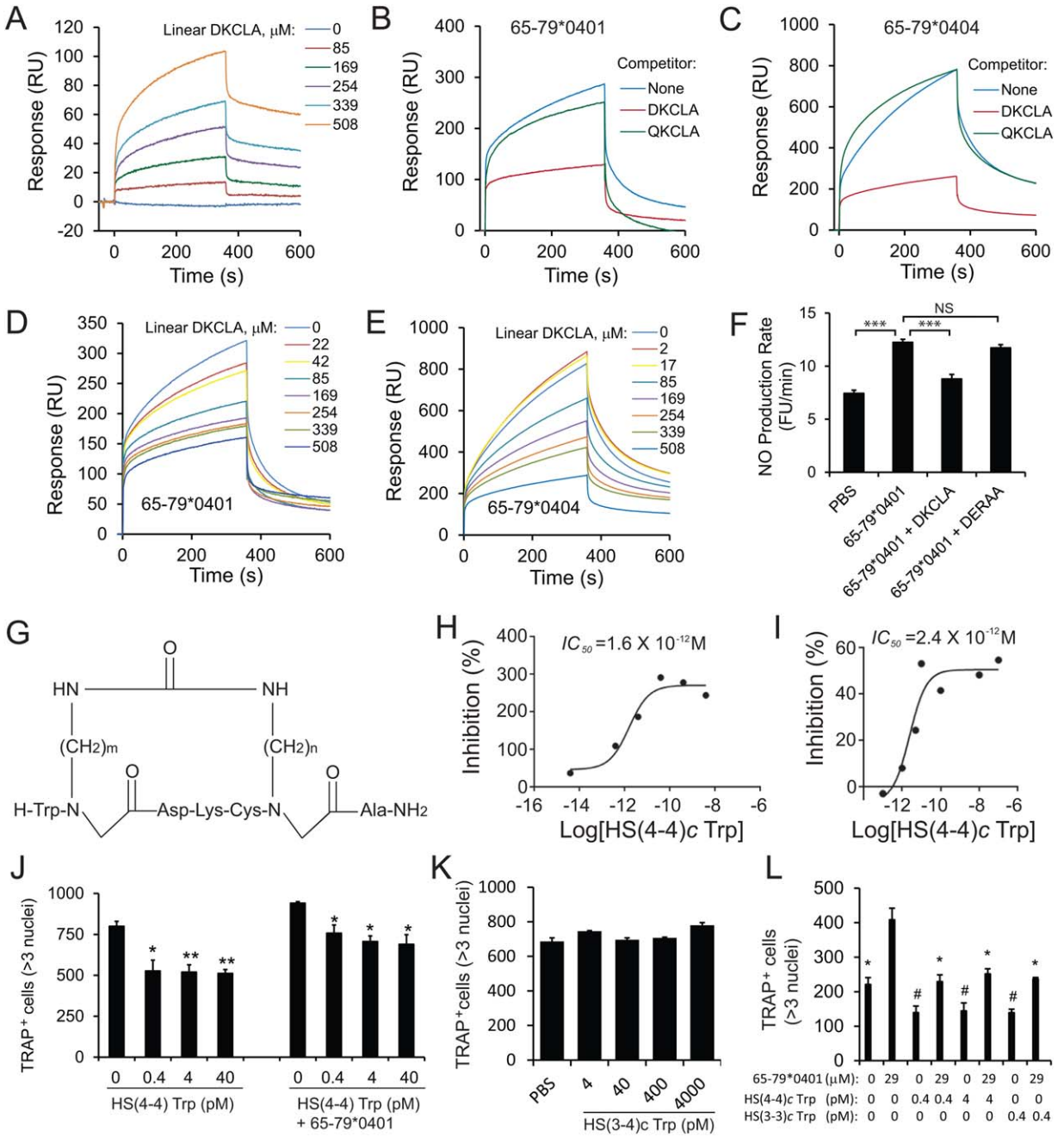

Figure 1. Shared epitope–antagonistic ligand (SEAL) activity in vitro. **A,** Interaction between linear DKCLA peptide and recombinant calreticulin. **B,** Specific inhibition of the interaction between SE ligand 65-79*0401 (171 μM) and calreticulin by linear DKCLA (508 μM). **C,** Specific inhibition of the interaction between SE ligand 65–79*0404 and calreticulin by linear DKCLA. **D,** Dose-response inhibition of the interaction between SE ligand 65–79*0401 (171 μM) and calreticulin by linear DKCLA. **E,** Dose-response inhibition of the interaction between SE ligand 65–79*0404 (169 μM) and calreticulin by linear DKCLA. **F,** Specific inhibition of SE ligand 65–79*0401 (57 μM)–activated nitric oxide (NO) signaling by linear DKCLA (170 μM). $*** = P < 0.001$ for the indicated comparisons. **G,** Structural formula of the cyclic DKCLA compound library. **H,** Dose-response curve showing the inhibitory effect of HS(4-4)c Trp on SE ligand 65–79*0401 (57 μM)–activated NO signaling. **I,** Competitive inhibition of SE ligand 65–79*0401 (229 μM) binding to calreticulin by HS(4-4)c Trp. **J,** Inhibition of unstimulated (left) and SE ligand 65–79*0401 (29 μM)–activated (right) osteoclastogenesis in primary mouse bone marrow cells (BMCs) by HS(4-4)c Trp, as indicated by tartrate-resistant acid phosphatase (TRAP)–positive cells. $* = P < 0.05$; $** = P < 0.01$ versus no treatment. **K,** No inhibition of osteoclastogenesis in mouse BMCs by HS(3-4)c Trp. **L,** Inhibition of SE ligand–activated osteoclastogenesis in human peripheral blood mononuclear cells by HS(4-4)c Trp and HS(3-3)c Trp. $* = P < 0.05$ versus 65–79*0401; $\# = P < 0.05$ versus phosphate buffered saline (PBS). Values in **F, J, K,** and **L** are the mean ± SEM. RU = resonance units; FU = fluorescence units; NS = not significant; IC_{50} = 50% inhibition concentration.

and 100 μg/ml of streptomycin in the presence of 10 ng/ml of M-CSF alone during the first 2 days, followed by 4 additional days in the presence of 10 ng/ml of M-CSF plus 20 ng/ml of RANKL.

Human OCs were differentiated from PBMCs derived from random blood donors, irrespective of their HLA–DRB1 genotype. Cells (2×10^5/well) were cultured in 48-well plates for 7 days in 100 ng/ml of M-CSF and 100 ng/ml of RANKL supplemented with 10% fetal calf serum–Dulbecco's modified Eagle's medium. To quantify the number of OCs, cultures were fixed and stained for tartrate-resistant acid phosphatase (TRAP) activity using an acid phosphatase kit (Kamiya Biomedical) according to the manufacturer's instructions. TRAP-positive multinucleated OCs (>3 nuclei) were counted using a tissue-culture inverted microscope.

CIA induction, in vivo compound administration, joint tissue studies, and imaging. DBA/1 mice were immunized with chicken type II collagen in CFA. Briefly, 50 μl of an emulsion containing 100 μg of chicken type II collagen in 25 μl of 0.05*M* acetic acid and 25 μl of CFA was injected intradermally at the base of the tail. Mice were injected intraperitoneally once a week for 7 weeks with 50 μl of either phosphate buffered saline (PBS), HS(4-4)c Trp, or HS(3-4)c Trp in PBS. Arthritis severity was determined using a 4-point visual scoring system for each paw, where 0 = no arthritis, 1 = swelling and redness confined to the digits, 2 = minor swelling and redness spreading from the digits to the distal paw, and 3 = major swelling and redness extending proximally from the paw.

Limbs were dissected and decalcified in 10% EDTA. After decalcification, the specimens were processed for paraffin embedding and serial sectioning. The histology sections were deparaffinized, rehydrated, and stained for TRAP activity using a commercial kit. To determine OC abundance, TRAP-positive multinucleated cells were counted. Data are reported as the mean ± SEM of the total number of OCs in the front and hind paws plus both knees.

For micro–computed tomography (micro-CT), the front and hind limbs were dissected, fixed in 10% formalin, and stored in 70% ethanol. Limbs were scanned ex vivo with a micro-CT system (eXplore Locus SP; GE Healthcare Canada) in distilled water. The protocol included a source powered at 80 kV and 80 μA. In addition to a 0.508-mm aluminum filter, an acrylic beam flattener was used to reduce beam-hardening artifact. Exposure time was defined as 1,600 msec/frame, with 400 views taken at increments of 0.5°. With 4 frames averaged and binning at 2×2, the images were reconstructed with an 18-μm isotropic voxel size.

Radiographs were obtained using a microradiography system (Faxitron) with the following operating settings: peak voltage of 27V, anode current of 2.5 mA, and an exposure time of 4.5 seconds. Coded radiographs were evaluated by an experienced rheumatologist (JH) who was blinded with regard to the treatment group. Bone erosions were scored on a scale of 0–5 for each of the 4 paws.

Docking models. BioMed CAChe 6.1 software (Fujitsu) was used for modeling of the interaction between ligands and the calreticulin P-domain. Cyclic peptidomimetics, which were loaded as flexible molecules, or the physiologically folded SE (residues 70–74 in the β-chain third allelic hypervariable region of HLA–DR4; PDB ID 2SEB) as a rigid conformation, were used as ligands. Rat calreticulin P-domain (PDB ID 1HHN) in its rigid conformation was used as receptor. Docking scores were calculated using BioMed CAChe 6.1 software. In all cases, the minimum potential energy and chemical bonds were determined for the most stable geometry.

Statistical analysis. Data are expressed as the mean ± SEM. Except where indicated otherwise, statistical analyses were performed using Student's *t*-test. *P* values less than 0.05 were considered significant.

RESULTS

DKCLA, a short linear synthetic peptide with SEAL properties. We identified a 5-mer peptide expressing the sequence DKCLA that interacted with calreticulin in an SPR-based assay (Figure 1A), and specifically inhibited the interaction between calreticulin and 15-mer peptide SE ligands corresponding to the 65–79 region coded by HLA–DRB1*04:01 (Figure 1B) or by DRB1*04:04 (Figure 1C) at a 50% inhibition concentration (IC_{50}) of 67 μM (Figure 1D) and 289 μM (Figure 1E), respectively. Additionally, linear DKCLA specifically blocked SE ligand–activated nitric oxide signaling (Figure 1F). Thus, the linear peptide DKCLA is a low-potency competitive inhibitor of the SE ligand, a functional characteristic referred to as SE-antagonistic ligand.

DKCLA peptidomimetics. Linear peptides are short-lived, and their biologic activity is further compromised by their random conformation in solution. Accordingly, as a peptide-stabilization strategy, we used a previously described procedure (21,22) to synthesize a library of backbone cDKCLA analogs, all carrying an identical primary sequence, but differing in the size of their ring (Figure 1G). Members of this library were screened in SE ligand–activated nitric oxide signaling assays to determine the relative SEAL potency of individual compounds in vitro. Of the 16 analogs tested, several were found to be exceptionally potent (e.g., the compounds HS[4-4]c Trp, HS[3-3]c Trp, and HS[6-4]c Trp) (Table 1), with IC_{50} values as low as $1.6 \times 10^{-12} M$ (Figure 1H). The lead compound HS(4-4)c Trp was tested in SPR assays, and was found to be a potent

Table 1. Differential inhibition of shared epitope–activated nitric oxide signaling by cDKCLA compounds*

cDKCLA compound	IC_{50}, *M*
HS(4-4)c Trp	1.6×10^{-12}
HS(3-3)c Trp	1.8×10^{-12}
HS(6-4)c Trp	6.3×10^{-9}
HS(4-6)c Trp	5.6×10^{-7}
HS(6-2)c Trp	7.7×10^{-7}
HS(3-4)c Trp	4.3×10^{-6}

* The cyclic DKCLA (cDKCLA) compounds examined are urea backbone cyclc peptidomimetics. IC_{50} = 50% inhibition concentration.

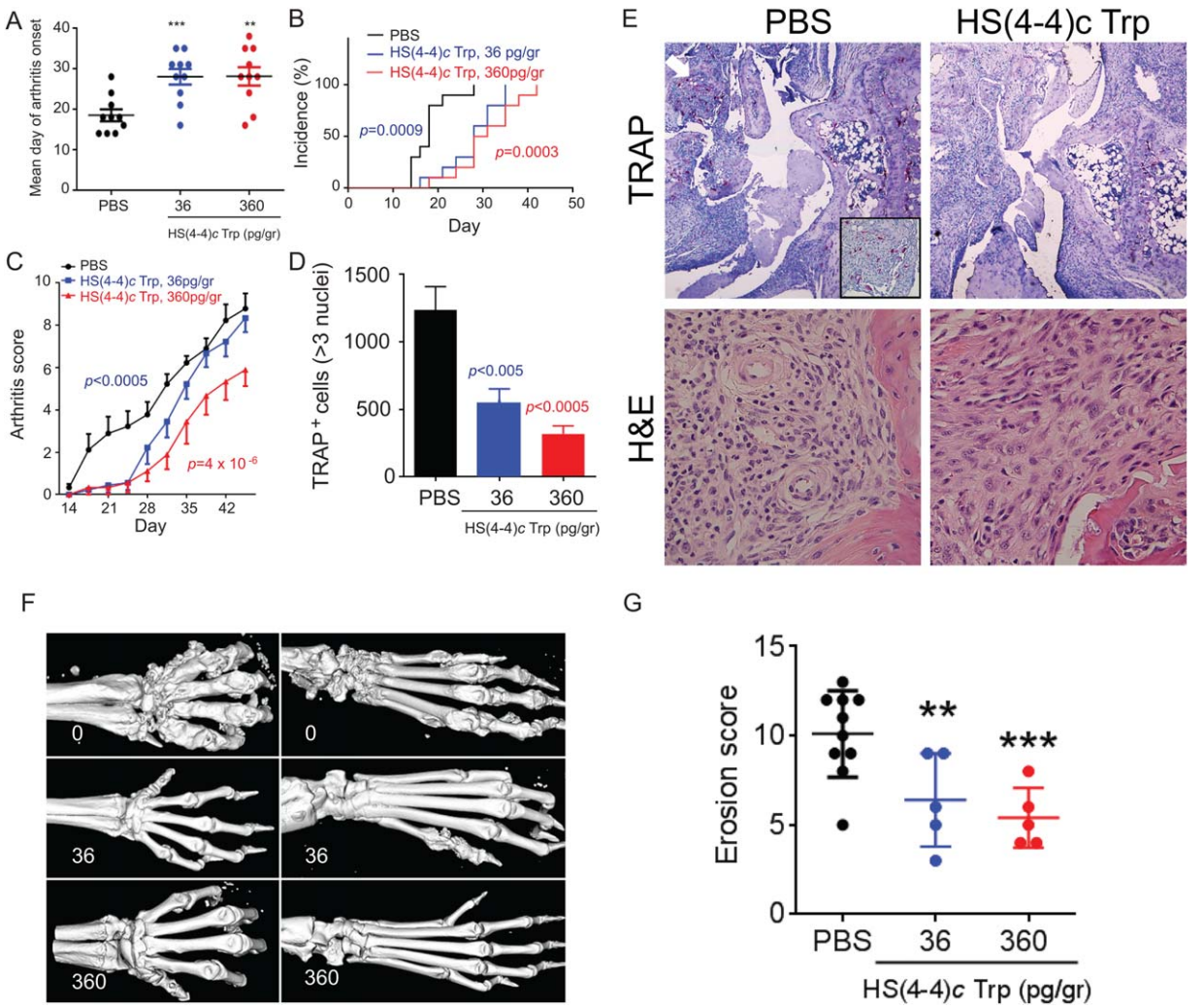

Figure 2. Amelioration of collagen-induced arthritis (CIA) by HS(4-4)c Trp. **A,** HS(4-4)c Trp at either 36 pg (blue) or 360 pg (red) per gram of body weight or phosphate buffered saline (PBS) (black) was administered intraperitoneally once a week for 7 weeks (n = 10 mice per group), and the day of arthritis onset was recorded. Each symbol represents a single mouse; horizontal lines with bars show the mean ± SEM. **B,** Incidence of arthritis over 45 days in the 3 treatment groups. **C,** Arthritis scores over 45 days in the 3 treatment groups. Values are the mean ± SEM. *P* values are versus PBS, by paired *t*-test. **D,** Synovial osteoclasts in the joints of mice in the 3 treatment groups, as indicated by tartrate-resistant acid phosphatase (TRAP)–positive cells. Values are the mean ± SEM of 5 mice per group. **E,** Histologic features of the wrist in mice with CIA treated with PBS or with 360 pg/gm of HS(4-4)c Trp. Sections were stained with TRAP (original magnification × 4) or with hematoxylin and eosin (H&E) (original magnification × 100). The region indicated by the white arrow at the top left corner of the TRAP-stained section from the mouse treated with PBS is shown at higher magnification in the **inset**. **F,** Micro–computed tomography images of the front (left) and hind (right) paws of mice with CIA treated with PBS (top), 36 pg/gm of HS(4-4)c Trp (middle), or 360 pg/gm of HS(4-4)c Trp (bottom). **G,** Bone erosion scores in the 3 treatment groups. Each symbol represents a single mouse; horizontal lines with bars show the mean ± SEM. In **A** and **G,** ** = $P < 0.01$; *** = $P < 0.001$ versus PBS.

competitive inhibitor of SE–calreticulin interaction, with an IC_{50} of $2.4 \times 10^{-12} M$ (Figure 1I). Thus, cDKCLA compound HS(4-4)c Trp is a 1,000,000 times more potent SEAL than the linear DKCLA peptide.

In vitro inhibition of OC differentiation by cDKCLA compounds. Since OCs play a key role in bone erosion–associated conditions, an attempt to inhibit these cells is a desirable therapeutic goal. Given the high SEAL potency of compounds HS(4-4)c Trp and HS(3-3)c Trp in signal transduction (Table 1), we carried out experiments to determine their effectiveness as OC inhibitors.

We found that in mouse cells (Figure 1J), the lead cDKCLA compound HS(4-4)c Trp very efficiently inhibited RANKL-activated OC differentiation. Moreover,

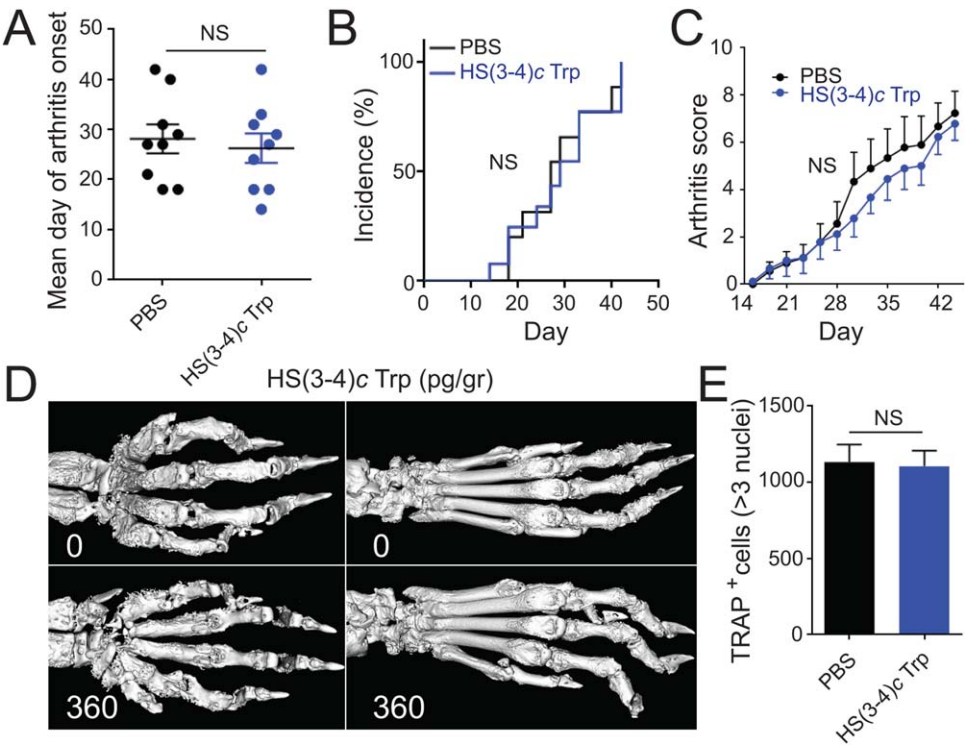

it significantly inhibited the incremental SE-activated OC differentiation. SEAL activity was found to be structure-specific, since the cDKCLA analog HS(3-4)c Trp, which carries an identical core amino acid sequence and only differs in the ring size, failed to inhibit OC differentiation (Figure 1K), consistent with its low inhibitory effect in signal transduction studies (Table 1). The antiosteoclastogenic effects of SEAL compounds HS(4-4)c and HS(3-3)c were tested in human PBMCs as well, and showed potent antiosteoclastogenic effects in the absence or presence of an exogenously added SE ligand (Figures 1J and L). The effect was found in both SE-positive and SE-negative PBMCs (results not shown). Additionally, preliminary data suggest that similar to their effect on PBMC-derived OCs, SEAL compounds inhibited signal transduction in human fibroblast-like synoviocytes irrespective of the SE status of the donor as well (results not shown).

Cyclic DKCLA analog–specific effects in vivo. The effects of SEAL compounds were studied in mice with CIA. As shown in Figure 2, mice injected intraperitoneally once a week with picogram doses of HS(4-4)c Trp experienced delayed onset (Figure 2A), lower incidence (Figure 2B), and significantly milder (Figure 2C) arthritis. Histologically, their joints showed less-abundant OCs in the synovial tissues (Figures 2D and E). Interestingly, although at the end of the treatment period (day 45 postimmunization) joint swelling was seen in all groups, pannus from PBS-treated mice showed greater lymphocytic infiltration than did the synovial tissue from HS(4-4)c Trp–treated mice (Figure 2E). Micro-CT and radiographic imaging demonstrated a lesser extent of bone destruction in the treated groups (Figures 2F and G). In contrast and consistent with its inactivity in vitro, the HS(3-4)c Trp analog had no effect on the day of arthritis onset (Figure 3A), the incidence of arthritis (Figure 3B), the disease severity (Figure 3C), the radiographic bone damage (Figure 3D), or the abundance of OCs in synovial tissues (Figure 3E).

No behavioral, physical, radiologic, or histologic aberrations were noticed in SEAL-treated mice as compared to controls. Untreated and treated mice (highest dosage 360 pg/gm of body weight weekly for up to 7 weeks) showed similar general health parameters (body weight, fur appearance, mobility, and food and water consumption rates).

As mentioned above, the compounds HS(4-4)c Trp and HS(3-4)c Trp share an identical core sequence, but differ slightly in their ring size. This minor structural

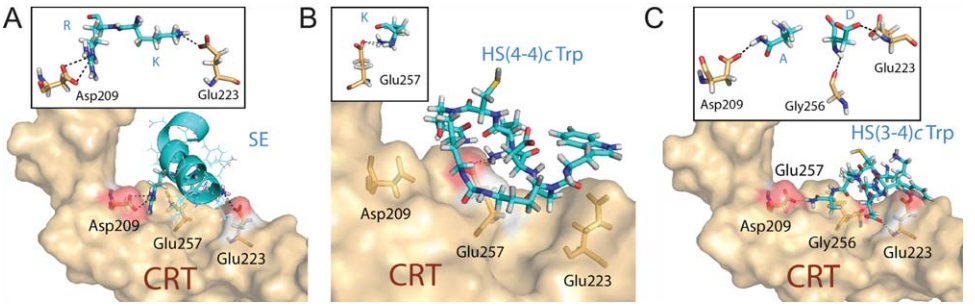

Figure 4. Docking models for **A,** the shared epitope (SE), **B,** the mimetic compound HS(4-4)c Trp, and **C**, the mimetic compound HS(3-4)c Trp. Ligands (blue) are docked to the calreticulin (CRT) surface (tan). Side chains of interacting calreticulin residues are highlighted in orange. Dotted lines represent chemical bonds. Red areas represent the surface of key calreticulin residues that interact with the ligands. **Insets** depict the chemical interactions. The calreticulin residues are identified in 3-letter format and the ligand residues in single-letter format.

dissimilarity nevertheless accounted for a major functional disparity between the 2 compounds. To gain better insights into the structure–function correlates of the 2 compounds, we docked them virtually onto a physiologically folded calreticulin P-domain (6), using BioMed CAChe 6.1 software.

Compounds HS(4-4)c Trp and HS(3-4)c Trp were both predicted to occupy the SE binding pocket (Figure 4); however, their respective chemical interactions within the binding pocket and their docking energies were distinct (Table 2). The lead SEAL compound HS(4-4)c Trp had a higher docking energy than the inactive analog HS(3-4)c Trp and engaged in a dual chemical bond with a single calreticulin residue (Glu^{257}). The inactive compound HS(3-4)c Trp, on the other hand, interacted weakly with 3 calreticulin residues: Asp^{209}, Glu^{223}, and Gly^{256}. For comparison, a similarly docked SE ligand in its native α-helical conformation had a single electrostatic bond with calreticulin residue Glu^{223} and a dual electrostatic bond with residue Asp^{209}. Thus, the inactive analog HS(3-4)c Trp, similar to the naturally folded SE ligand, was predicted to generate a "bridging" effect across the SE binding pocket, while the SEAL compound HS(4-4)c Trp displayed a strong focal interaction with calreticulin residue Glu^{257} at the center of that pocket (Figure 4). Taken together, the data in Figure 4 and Table 2 indicate that despite their nearly identical chemical structure, the 2 functionally disparate compounds displayed distinct molecular interactions with the SE binding site on calreticulin.

DISCUSSION

The main significance of the findings reported herein is the identification of the SE/calreticulin pathway as a novel therapeutic target. To date, treatment modalities in RA have targeted cytokines, their receptors, or

Table 2. Ligand–calreticulin docking characteristics*

Ligand (core aa sequence)	Docking energy, kcal/mole	Interacting residues†		Distance, Å	Chemical bond
		Calreticulin	Ligand		
SE (^{70}QKRAA^{74})	−207	Asp^{209}	R^{72}	3.5	ESB
		Asp^{209}	R^{72}	3.5	ESB
		Glu^{223}	K^{71}	3.2	ESB
HS(4-4)c Trp (DKCLA)	−109	Glu^{257}	K	2.1	HB
		Glu^{257}	K	2.6	ESB
HS(3-4)c Trp (DKCLA)	−21.9	Asp^{209}	A	1.8	HB
		Glu^{223}	D	2.1	HB
		Gly^{256}	D	2.1	HB

* Two urea backbone cyclic peptidomimetics were examined: HS(4-4)c Trp and HS(3-4)C Trp. SE = shared epitope; ESB = electrostatic bond; HB = hydrogen bond.
† Calreticulin residues are shown in the 3-letter format, and the numbers correspond to the location of the given amino acid (aa) residue in the calreticulin sequence. Ligand residues are shown in the single-letter format, and the numbers correspond to the location of the amino acid residue in the DRβ chain sequence.

other players in the immune-activated final common pathway. Due to their involvement in "downstream" segments of RA pathogenesis, these targets are often redundant and/or nonspecific. As a result, current treatment modalities are often ineffective, and/or they carry high rates of side effects, mainly infection (23). The advantage of a SEAL-based therapeutic approach over current or emerging drugs is that it addresses an unmet need by offering a potent intervention strategy that specifically targets an "upstream" segment of the pathogenic cascade.

The compounds described herein were found to be highly potent, both in vitro and in vivo. For example, compounds HS(4-4)c Trp and HS(3-3)c Trp competitively blocked SE signaling effects and inhibited OC differentiation at low picomolar concentrations, a 1,000-fold higher potency than JAK inhibitors (24). The in vivo effect of compound HS(4-4)c Trp, likewise, was much more potent than that of emerging drugs reported to exert therapeutic efficacy in CIA at doses in the milligram-per-kilogram range (24–26). In contrast, compound HS(4-4)c Trp described herein achieved disease-amelioration effects at doses in the nanogram-per-kilogram range, a 1,000,000-fold higher potency.

Interestingly, despite its seemingly modest anti-osteoclastogenic effect in vitro (Figures 1J and L), SEAL compound HS(4-4)c Trp was highly effective in diminishing tissue OCs when administered in vivo to mice with CIA (Figure 2D). The likely explanation for the apparent discrepancy is that in vitro assays do not accurately replicate the cellular events that take place in vivo. Specifically in this case, in vitro OC-differentiation assays were carried out using mouse BMCs (Figure 1J) or human PBMCs (Figure 1L), while in vivo, the abundance of OCs was determined within mouse synovial tissue, which represents a different cellular milieu. Second, in vitro OC-differentiation protocols used selected pro-osteoclastogenic factors (M-CSF and RANKL), whereas the in vivo process involved additional pro-osteoclastogenic and antiosteoclastogenic factors. Third, the in situ concentrations of RANKL and M-CSF are likely to be lower than those used to artificially stimulate robust OC differentiation in vitro.

SEAL compound–treated CIA mice showed delayed arthritis onset and decreased incidence; however, both the treated and control groups eventually developed joint swelling and reached equivalent disease incidence. This observation is consistent with our previous studies demonstrating that the arthritogenic effect of SE agonist ligands affect joint swelling in the early phase of CIA, but less so in the chronic phase (12,13). The mechanistic basis of the differential effect on early versus late joint swelling is unknown, but is likely to be related to the fact that the early and late stages of CIA are distinct in their pathogenic mechanisms and in the degree of their responsiveness to therapeutic interventions (27–31). Similarly consistent with our previous findings with SE agonist ligands (12,13), which demonstrated a disproportionate impact on bone erosions relative to their effects on joint swelling, the SEAL compound reversed this trend by affecting primarily bone damage. Such a differential effect is not without precedent, as disparate severities of joint inflammation versus bone erosion have previously been reported in experimental arthritis models (32,33) as well as in RA in humans (34). Better understanding of the mechanisms governing bone selectivity by SEAL compounds could provide important new insights into the pathogenic mechanisms that specifically underlie inflammation versus bone damage.

It should be pointed out that SEAL compounds inhibited basal osteoclastogenesis in vitro even in the absence of the SE ligand and ameliorated CIA in mice that do not carry SE-coding MHC class II alleles. Therefore, consistent with the SE ligand theory (for a discussion, see refs. 35 and 36), it is reasonable to propose the existence of a physiologic calreticulin-binding ligand capable of OC activation during healthy bone remodeling. There are several physiologic ligands that the SE ligand could potentially mimic. For example, circulating levels of adiponectin, a known calreticulin ligand (37), have been shown to correlate with the extent of radiographic bone damage in RA (38). It is noteworthy that adiponectin facilitates Th17 polarization (39) and can activate OCs (for review, see ref. 40). Thrombospondin 1, likewise a well-characterized calreticulin ligand (41) that is implicated in RA pathogenesis (42,43), facilitates Th17 polarization (44) and activates OCs (45).

Obviously, identification of the specific physiologic calreticulin ligand that the SE may be mimicking requires further study. However, irrespective of the identity of that physiologic ligand, the model proposed here hypothesizes that the SE may facilitate OC activation and bone damage by mimicking a putative physiologic ligand. Accordingly, SEAL compounds may ameliorate OC activation and arthritis through competitive inhibition of a physiologic ligand, independently of the presence or absence of an SE ligand. This model further posits that individuals with SE-coding HLA–DRB1 alleles are at higher risk of developing erosive arthritis due to the high abundance of cell surface SE-expressing HLA–DR molecules that mimic the physiologic OC-activating ligand. Under certain genetic and environmental circumstances, the SE ligand may overactivate the innate pathway, with resultant

excessive activation of OCs. In this context, it is worth noting that SE-associated bone damage is not unique to RA, as SE-coding HLA–DRB1 alleles have been shown to associate with accelerated bone erosion in patients with psoriatic arthritis (46), patients with periodontal disease (47), and patients with SLE (48).

Beyond offering new insights into the pathogenesis of bone damage in arthritis, our findings illustrate the therapeutic targetability of the SE/calreticulin pathway by highly specific, rationally designed SEAL compounds. The compounds presented here were highly potent, both in vitro and in vivo, and showed exquisite structure–activity relationships. These facts could facilitate future compound optimization efforts. From a medicinal chemistry perspective, it is also worth noting that the cysteine residue does not appear to play a role in the antagonist's interaction model with calreticulin (Figure 4 and Table 2). Additionally, since the inactive compound HS(3-4)c Trp contains cysteine in the same position as the active compounds HS(4-4)c Trp and HS(3-3)c Trp, the cysteine residue, including its thiol side chain, is unlikely to play a functional role in the biologic effects of these compounds.

The new strategy presented herein may be safer than using prevailing drugs because of the unique role played by this pathway at an "upstream" phase in RA pathogenesis. The SE is the single most significant risk factor for RA. It determines susceptibility, severity, and disease penetrance (49). Thus, different from effector cytokines or intracellular enzymes, this pathway is involved in the early segments of disease etiology and pathogenesis. Targeting such an "upstream" pathway might be more effective and would likely produce fewer side effects.

In conclusion, the findings of this study suggest that SEAL compounds could be useful tools for examining the mechanisms governing bone erosion in various conditions, including RA. Furthermore, the results provide a rationale and early medicinal information that could help in the development of specific, potent, safe, and inexpensive drugs for arthritis and other erosive bone conditions.

AUTHOR CONTRIBUTIONS

All authors were involved in drafting the article or revising it critically for important intellectual content, and all authors approved the final version to be published. Dr. Holoshitz had full access to all of the data in the study and takes responsibility for the integrity of the data and the accuracy of the data analysis.

Study conception and design. Ling, Liu, Fu, Gilon, Holoshitz.
Acquisition of data. Ling, Liu, Fu, Colletta, Gilon.
Analysis and interpretation of data. Ling, Liu, Gilon, Holoshitz.

REFERENCES

1. Gregersen PK, Silver J, Winchester RJ. The shared epitope hypothesis: an approach to understanding the molecular genetics of susceptibility to rheumatoid arthritis. Arthritis Rheum 1987; 30:1205–13.
2. Gonzalez-Gay MA, Garcia-Porrua C, Hajeer AH. Influence of human leukocyte antigen-DRB1 on the susceptibility and severity of rheumatoid arthritis. Semin Arthritis Rheum 2002;31:355–60.
3. Mattey DL, Hassell AB, Dawes PT, Cheung NT, Poulton KV, Thomson W, et al. Independent association of rheumatoid factor and the HLA–DRB1 shared epitope with radiographic outcome in rheumatoid arthritis. Arthritis Rheum 2001;44:1529–33.
4. Plant MJ, Jones PW, Saklatvala J, Ollier WE, Dawes PT. Patterns of radiological progression in early rheumatoid arthritis: results of an 8 year prospective study. J Rheumatol 1998;25:417–26.
5. Weyand CM, Goronzy JJ. Disease mechanisms in rheumatoid arthritis: gene dosage effect of HLA-DR haplotypes. J Lab Clin Med 1994;124:335–8.
6. Ling S, Cheng A, Pumpens P, Michalak M, Holoshitz J. Identification of the rheumatoid arthritis shared epitope binding site on calreticulin. PLoS One 2010;5:e11703.
7. De Almeida DE, Ling S, Pi X, Hartmann-Scruggs AM, Pumpens P, Holoshitz J. Immune dysregulation by the rheumatoid arthritis shared epitope. J Immunol 2010;185:1927–34.
8. Ling S, Cline EN, Haug TS, Fox DA, Holoshitz J. Citrullinated calreticulin potentiates rheumatoid arthritis shared epitope signaling. Arthritis Rheum 2013;65:618–26.
9. Ling S, Lai A, Borschukova O, Pumpens P, Holoshitz J. Activation of nitric oxide signaling by the rheumatoid arthritis shared epitope. Arthritis Rheum 2006;54:3423–32.
10. Ling S, Li Z, Borschukova O, Xiao L, Pumpens P, Holoshitz J. The rheumatoid arthritis shared epitope increases cellular susceptibility to oxidative stress by antagonizing an adenosine-mediated anti-oxidative pathway. Arthritis Res Ther 2007;9:R5.
11. Ling S, Pi X, Holoshitz J. The rheumatoid arthritis shared epitope triggers innate immune signaling via cell surface calreticulin. J Immunol 2007;179:6359–67.
12. Fu J, Ling S, Liu Y, Yang J, Naveh S, Hannah M, et al. A small shared epitope-mimetic compound potently accelerates osteoclast-mediated bone damage in autoimmune arthritis. J Immunol 2013;191:2096–103.
13. Holoshitz J, Liu Y, Fu J, Joseph J, Ling S, Colletta A, et al. An HLA-DRB1-coded signal transduction ligand facilitates inflammatory arthritis: a new mechanism of autoimmunity. J Immunol 2013;190:48–57.
14. Gravallese EM, Manning C, Tsay A, Naito A, Pan C, Amento E, et al. Synovial tissue in rheumatoid arthritis is a source of osteoclast differentiation factor. Arthritis Rheum 2000;43:250–8.
15. Schett G, Gravallese E. Bone erosion in rheumatoid arthritis: mechanisms, diagnosis and treatment. Nat Rev Rheumatol 2012; 8:656–64.
16. De Punder YM, van Riel PL. Rheumatoid arthritis: understanding joint damage and physical disability in RA. Nat Rev Rheumatol 2011;7:260–1.
17. Le Goff B, Berthelot JM, Maugars Y, Heymann D. Osteoclasts in RA: diverse origins and functions. Joint Bone Spine 2013;80: 586–91.
18. Kim HR, Kim KW, Kim BM, Jung HG, Cho ML, Lee SH. Reciprocal activation of CD4+ T cells and synovial fibroblasts by stromal cell–derived factor 1 promotes RANKL expression and osteoclastogenesis in rheumatoid arthritis. Arthritis Rheum 2014;66:538–48.
19. Kotake S, Udagawa N, Takahashi N, Matsuzaki K, Itoh K, Ishiyama S, et al. IL-17 in synovial fluids from patients with rheumatoid arthritis is a potent stimulator of osteoclastogenesis. J Clin Invest 1999;103:1345–52.

20. Sato K, Suematsu A, Okamoto K, Yamaguchi A, Morishita Y, Kadono Y, et al. Th17 functions as an osteoclastogenic helper T cell subset that links T cell activation and bone destruction. J Exp Med 2006;203:2673–82.
21. Hurevich M, Tal-Gan Y, Klein S, Barda Y, Levitzki A, Gilon C. Novel method for the synthesis of urea backbone cyclic peptides using new Alloc-protected glycine building units. J Pept Sci 2010;16:178–85.
22. Naveh S, Tal-Gan Y, Ling S, Hoffman A, Holoshitz J, Gilon C. Developing potent backbone cyclic peptides bearing the shared epitope sequence as rheumatoid arthritis drug-leads. Bioorg Med Chem Lett 2012;22:493–6.
23. Furst DE. The risk of infections with biologic therapies for rheumatoid arthritis. Semin Arthritis Rheum 2010;39:327–46.
24. Fridman JS, Scherle PA, Collins R, Burn TC, Li Y, Li J, et al. Selective inhibition of JAK1 and JAK2 is efficacious in rodent models of arthritis: preclinical characterization of INCB028050. J Immunol 2010;184:5298–307.
25. Stump KL, Lu LD, Dobrzanski P, Serdikoff C, Gingrich DE, Dugan BJ, et al. A highly selective, orally active inhibitor of Janus kinase 2, CEP-33779, ablates disease in two mouse models of rheumatoid arthritis. Arthritis Res Ther 2011;13:R68.
26. William AD, Lee AC, Poulsen A, Goh KC, Madan B, Hart S, et al. Discovery of the macrocycle (9E)-15-(2-(pyrrolidin-1-yl) ethoxy)-7,12,25-trioxa-19,21,24-triaza-tetracyclo[18. 3.1.1(2,5).1(14,18)]hexacosa-1(24),2,4,9,14(26),15,17,20,22-nonaene (SB1578), a potent inhibitor of janus kinase 2/fms-like tyrosine kinase-3 (JAK2/FLT3) for the treatment of rheumatoid arthritis. J Med Chem 2012;55:2623–40.
27. Svendsen P, Andersen CB, Willcox N, Coyle AJ, Holmdahl R, Kamradt T, et al. Tracking of proinflammatory collagen-specific T cells in early and late collagen-induced arthritis in humanized mice. J Immunol 2004;173:7037–45.
28. Merky P, Batsalova T, Bockermann R, Dzhambazov B, Sehnert B, Burkhardt H, et al. Visualization and phenotyping of proinflammatory antigen-specific T cells during collagen-induced arthritis in a mouse with a fixed collagen type II-specific transgenic T-cell receptor β-chain. Arthritis Res Ther 2010;12:R155.
29. Miellot-Gafsou A, Biton J, Bourgeois E, Herbelin A, Boissier MC, Bessis N. Early activation of invariant natural killer T cells in a rheumatoid arthritis model and application to disease treatment. Immunology 2010;130:296–306.
30. Abreu JR, Dontje W, Krausz S, de Launay D, van Hennik PB, van Stalborch AM, et al. A Rac1 inhibitory peptide suppresses antibody production and paw swelling in the murine collagen-induced arthritis model of rheumatoid arthritis. Arthritis Res Ther 2010;12:R2.
31. Bruhl H, Cihak J, Niedermeier M, Denzel A, Rodriguez Gomez M, Talke Y, et al. Important role of interleukin-3 in the early phase of collagen-induced arthritis. Arthritis Rheum 2009;60: 1352–61.
32. Joosten LA, Helsen MM, Saxne T, van de Loo FA, Heinegard D, van den Berg WB. IL-1$\alpha\beta$ blockade prevents cartilage and bone destruction in murine type II collagen-induced arthritis, whereas TNF-α blockade only ameliorates joint inflammation. J Immunol 1999;163:5049–55.
33. Binder NB, Puchner A, Niederreiter B, Hayer S, Leiss H, Bluml S, et al. Tumor necrosis factor–inhibiting therapy preferentially targets bone destruction but not synovial inflammation in a tumor necrosis factor–driven model of rheumatoid arthritis. Arthritis Rheum 2013;65:608–17.
34. Backhaus M, Burmester GR, Sandrock D, Loreck D, Hess D, Scholz A, et al. Prospective two year follow up study comparing novel and conventional imaging procedures in patients with arthritic finger joints. Ann Rheum Dis 2002;6:895–904.
35. De Almeida DE, Holoshitz J. MHC molecules in health and disease: at the cusp of a paradigm shift. Self Nonself 2011;2:43–8.
36. Holoshitz J. The quest for better understanding of HLA-disease association: scenes from a road less travelled by. Discov Med 2013;16:93–101.
37. Takemura Y, Ouchi N, Shibata R, Aprahamian T, Kirber MT, Summer RS, et al. Adiponectin modulates inflammatory reactions via calreticulin receptor-dependent clearance of early apoptotic bodies. J Clin Invest 2007;117:375–86.
38. Giles JT, van der Heijde DM, Bathon JM. Association of circulating adiponectin levels with progression of radiographic joint destruction in rheumatoid arthritis. Ann Rheum Dis 2011;70:1562–8.
39. Jung MY, Kim HS, Hong HJ, Youn BS, Kim TS. Adiponectin induces dendritic cell activation via PLCγ/JNK/NF-κB pathways, leading to Th1 and Th17 polarization. J Immunol 2012;188:2592–601.
40. Kanazawa I. Adiponectin in metabolic bone disease. Curr Med Chem 2012;19:5481–92.
41. Goicoechea S, Orr AW, Pallero MA, Eggleton P, Murphy-Ullrich JE. Thrombospondin mediates focal adhesion disassembly through interactions with cell surface calreticulin. J Biol Chem 2000;275:36358–68.
42. Vallejo AN, Mugge LO, Klimiuk PA, Weyand CM, Goronzy JJ. Central role of thrombospondin-1 in the activation and clonal expansion of inflammatory T cells. J Immunol 2000;164:2947–54.
43. Rico MC, Rough JJ, Del Carpio-Cano FE, Kunapuli SP, DeLa Cadena RA. The axis of thrombospondin-1, transforming growth factor β and connective tissue growth factor: an emerging therapeutic target in rheumatoid arthritis. Curr Vasc Pharmacol 2010; 8:338–43.
44. Yang K, Vega JL, Hadzipasic M, Schatzmann Peron JP, Zhu B, Carrier Y, et al. Deficiency of thrombospondin-1 reduces Th17 differentiation and attenuates experimental autoimmune encephalomyelitis. J Autoimmun 2009;32:94–103.
45. Carron JA, Walsh CA, Fraser WD, Gallagher JA. Thrombospondin promotes resorption by osteoclasts in vitro. Biochem Biophys Res Commun 1995;213:1017–25.
46. Korendowych E, Dixey J, Cox B, Jones S, McHugh N. The influence of the HLA-DRB1 rheumatoid arthritis shared epitope on the clinical characteristics and radiological outcome of psoriatic arthritis. J Rheumatol 2003;30:96–101.
47. Marotte H, Farge P, Gaudin P, Alexandre C, Mougin B, Miossec P. The association between periodontal disease and joint destruction in rheumatoid arthritis extends the link between the HLA-DR shared epitope and severity of bone destruction. Ann Rheum Dis 2006;65:905–9.
48. Chan MT, Owen P, Dunphy J, Cox B, Carmichael C, Korendowych E, et al. Associations of erosive arthritis with anticyclic citrullinated peptide antibodies and MHC Class II alleles in systemic lupus erythematosus. J Rheumatol 2008;35:77–83.
49. Jawaheer D, Thomson W, MacGregor AJ, Carthy D, Davidson J, Dyer PA, et al. "Homozygosity" for the HLA–DR shared epitope contributes the highest risk for rheumatoid arthritis concordance in identical twins. Arthritis Rheum 1994;37:681–6.